

NASA Technical Paper 1680

LOAN COPY RETURN
APWL TECHNICAL LIB
KIRTLAND AFB, N.M.

0067747



TECH LIBRARY KAFB, NM

Design and Cold-Air Test of Single-Stage Uncooled Core Turbine With High Work Output

Thomas P. Moffitt, Edward M. Szanca,
Warren J. Whitney, and Frank P. Behning

JUNE 1980

NASA

X
I



NASA Technical Paper 1680

Design and Cold-Air Test of Single-Stage Uncooled Core Turbine With High Work Output

Thomas P. Moffitt, Edward M. Szanca,
Warren J. Whitney, and Frank P. Behning
*Lewis Research Center
Cleveland, Ohio*



National Aeronautics
and Space Administration

**Scientific and Technical
Information Office**

1980

Summary

The cold-air performance of a solid version of a 50.8 centimeter (20-in.) single-stage turbine designed for high temperature core engine application is presented herein. The turbine was designed to produce an equivalent specific work output of 76.84 joules per gram (33.01 Btu/lb) at an engine turbine tip speed of 579.1 meters per second (1900 ft/sec). The turbine had relatively thick leading and trailing edge blading, low aspect ratio and high thickness to chord ratio.

The turbine was tested over a range of total-to-total pressure ratios from 2.0 to 4.0 and a range of speeds from 60 to 110 percent of design. At design speed and pressure ratio, the turbine efficiency was 0.886, which is 0.6 point lower than the design value of 0.892. The corresponding mass flow was 4.0 percent greater than design. Because of the flat vane exit angle (73° from axial), the 4 percent excess flow represents a misalignment of the vanes of only 0.7° . This underscores the care required to properly match this type of turbine to the rest of the engine.

Very little mixing occurred in a plane midway between the vanes and blades. Calculations from vane exit tip static pressures indicate a probable 14° unsteady change in incidence as the rotor blades pass each vane exit passage. The effect on blade incidence loss is unknown, but it could be significant.

Introduction

Future turbofan engines for commercial and some military aircraft will use higher bypass ratios, pressures, and temperatures than present engines. The "core" turbines associated with these engines will have to be cooled and are characterized by their relatively small-sized blading (high hub-to-tip-radius ratio) and low aspect ratio.

The resultant high end wall and secondary flow contributions to loss in conjunction with the required coolant flows complicate the designer's problem of evolving highly efficient, long life turbines. Consequently, many studies are underway at the Lewis Research Center and elsewhere to determine the effect of these unique characteristics on core turbine performance and to properly allow for them in design programs.

The engine designer must make a choice between a one-stage versus a two-stage core turbine. The major

trade-off differences between the two are the higher efficiency of the two-stage and the fewer parts of the one-stage turbine. These differences have counterbalancing effects on initial cost, operating cost, and repair cost. The selection depends on the particular engine involved, its anticipated use, and ultimately becomes the designer's choice. There is presently no demonstrated advantage of one over the other.

A two-stage turbine was initially selected for study at Lewis primarily because it is more conservative than a corresponding one-stage turbine due to lower blade speeds and Mach numbers. The design inlet temperature and pressure were 2200 K (3960° R) and 386 N/cm² abs (560 psia), respectively. The blade tip speed was 444 meters per second (1456 ft/sec), and the maximum flow Mach number from the vane hub was 0.81. The first stage of the two-stage turbine was extensively tested at Lewis (refs. 1 and 2) and under contract by General Electric (refs. 3 to 6). Both solid and full-film cooled versions were tested at a turbine inlet temperature of 783 K (1410° R). The geometric constraints involved in the design resulted in a solid turbine efficiency of about 0.88. The full-film cooled versions resulted in losses of up to one-half point in efficiency for each percent coolant added, which is very significant. Film cooling of the latter portion of the blade suction surface where high Mach numbers exist was responsible for the majority of the losses.

A second generation single-stage turbine was then designed to extract the same amount of work as the two-stage turbine described previously. The same inlet conditions of temperature and pressure were used. Blade tip speed was increased to 579.1 meters per second (1900 ft/sec), and the maximum flow Mach number from the vane hub increased to 1.20. Also, flow was reduced by 25 percent to represent a higher bypass ratio consistent with future engines. The resultant vane mean exit flow angle (measured from axial direction) increased from 67.0° to 73.0° . A solid version of this turbine was then tested at Lewis to determine the base uncooled performance.

This report covers the design and the cold-air test results of the solid single-stage turbine. The tests were conducted at an inlet pressure of 24.13 N/cm² (35 psia) and an inlet temperature of 378 K (680° R) and over a range of pressure ratio and speed. Results are given in terms of flow, torque, work output, efficiency, and outlet flow angle as a function of overall pressure ratio and speed.

Symbols

A	area, cm ² ; ft ²
b	vane or blade height, cm; in.
c	chord length, cm; in.
D	diameter, cm; in.
g	force-mass conversion constant, 1.0 (32.174 ft/sec ²)
Δh	specific work, J/g; Btu/lbm
J	mechanical equivalent of heat, 1.0 (778.16 ft-lb/Btu)
N	rotative speed, rad/sec
p	pressure, N/cm ² abs; psia
R	gas constant, 288 J/(kg)(K); 53.527 ft-lb/(lb)(°R) for test conditions
s	spacing, m; ft
T	absolute temperature, K; °R
U	blade velocity, m/sec; ft/sec
V	absolute gas velocity, m/sec; ft/sec
W	relative gas velocity, m/sec; ft/sec
w	mass flow, kg/sec; lbm/sec
α	absolute gas flow angle measured from axial direction, deg
β	relative gas flow angle measured from axial direction, deg
γ	ratio of specific heats, 1.398 for test conditions
δ	ratio of inlet total pressure to U.S. standard sea-level pressure, p_0/p^*
ϵ	function of γ used in relating parameters to those using air inlet conditions at U.S. standard sea-level conditions, $(0.73959/\gamma)[(\gamma+1)/2]^{\gamma/(\gamma-1)}$
η	total efficiency (based on inlet-total to exit-total) pressure ratio
θ_{cr}	squared ratio of critical velocity at turbine inlet to critical velocity at U.S. standard sea-level air $(V_{cr}/V_{cr}^*)^2$
τ	torque, N-m, ft-lb

Subscripts:

b	blade
cr	condition corresponding to Mach number of unity
l	local condition
m	mean section
t	tip section
u	tangential component
v	vane

x	axial component
0	station at turbine inlet
1	station at stator exit
2	station at turbine exit

Superscripts:

'	absolute total state
*	U.S. standard sea-level conditions (temperature equal to 288.15 K (518.7° R), pressure equal to 10.13 N/cm ² abs (14.696 psia))

Turbine Description

The design operating values for the single-stage core turbine are summarized in table I. Also shown are corresponding air-equivalent design parameters used for the solid version tested herein. The equivalent conditions were derived assuming no coolant-air effects. The high required equivalent work output noted from table I results in an overall total-to-total pressure ratio of 3.00 for the indicated efficiency value of 0.892. The only efficiency referred to in this report is "total" efficiency and is based on the ideal work related to total-to-total pressure ratio across the turbine. Because of property differences, the corresponding equivalent pressure ratio noted in table I for the cold conditions was 3.44 for the same equivalent ideal work.

The velocity diagrams evolved to meet the design aerodynamic requirements are shown in figure 1. All quantities represent the free stream uniform flow conditions before and after each blade row. The maximum critical velocity ratio is 1.16 (Mach number of 1.20) and occurs at the exit of the vane hub. The maximum blade relative critical velocity ratio is 1.08 and occurs at the exit of the blade tip. The exit swirl angle amounts to about 24° and is fairly constant from hub to tip. It is interesting to note the flat vane exit flow angle (73° from axial) typical of this type of turbine requirement.

Test turbine geometry values are summarized in table II. The vane and blade coordinates are shown in tables III and IV. The vanes and blades are characterized by blunt leading and trailing edges to allow for cooling, low aspect ratio, and high thickness to chord ratio. The design rotor tip running clearance was 0.030 centimeter (0.012 in.) and represents 0.8 percent of the blade height. The turbine was designed for free-vortex conditions. However, to meet the variation in free-stream vane exit angle of 2.6° from hub to tip (from velocity diagrams), the physical vane exit would have to be twisted only 1.5° because of blockage effect differences between the hub and tip. Therefore, the

stator was fabricated with untwisted vanes of constant mean-section profile, ignoring the 1.5° of twist. The blades were twisted about 9° from hub to tip as noted from table III.

The stage work factor ($gJ \Delta h/U_m^2$) of the turbine was 1.94. This value and figure 18 of reference 7 were used to predict a base efficiency of 0.920 for a long bladed turbine with negligible clearance and trailing edge blockage effects. Corrections were then made for clearance (1.4 points), aspect ratio (0.5 point), and trailing edge blockage (0.9 points) effects from available literature. The resulting design efficiency value was 0.892, which represents about a 3-point penalty due to geometric constraints.

Vane and blade design surface velocity distributions are shown in figures 2 and 3, respectively, for the hub, mean and tip locations. The vanes were designed for nearly constant acceleration from inlet to exit with very little surface diffusion (deceleration). The blades were designed to minimize suction surface diffusion at the expense of allowing considerable pressure surface diffusion, particularly in the hub region. This also minimized the maximum suction surface flow velocities to essentially exit flow values.

A photograph of the stator and rotor installed in the test facility is shown in figure 4. The stator consisted of 36 vanes and there were 64 blades on the rotor.

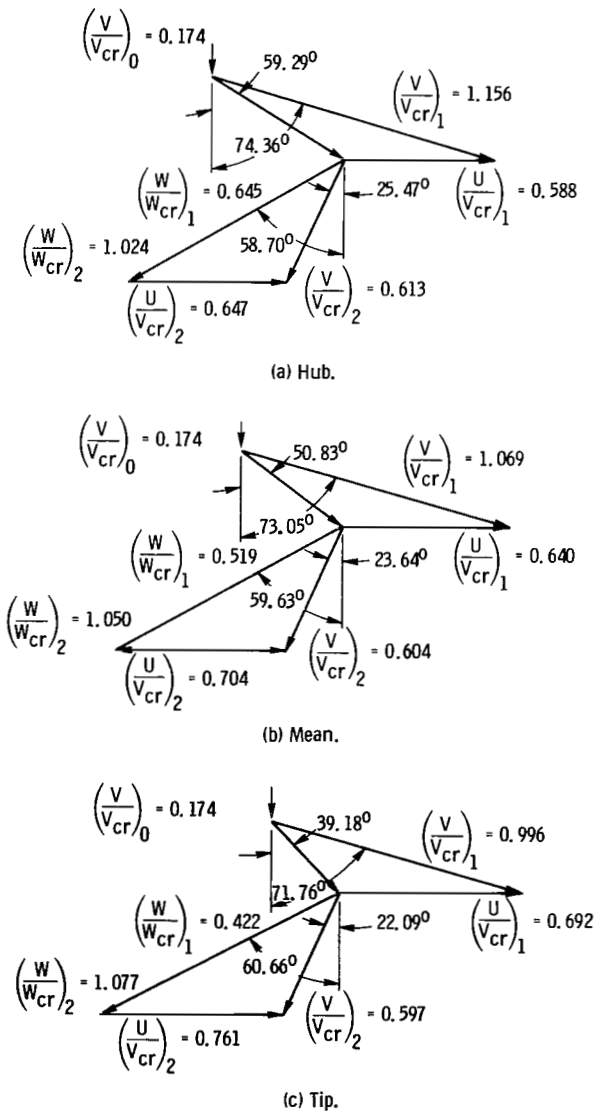


Figure 1. - Turbine design velocity diagrams.

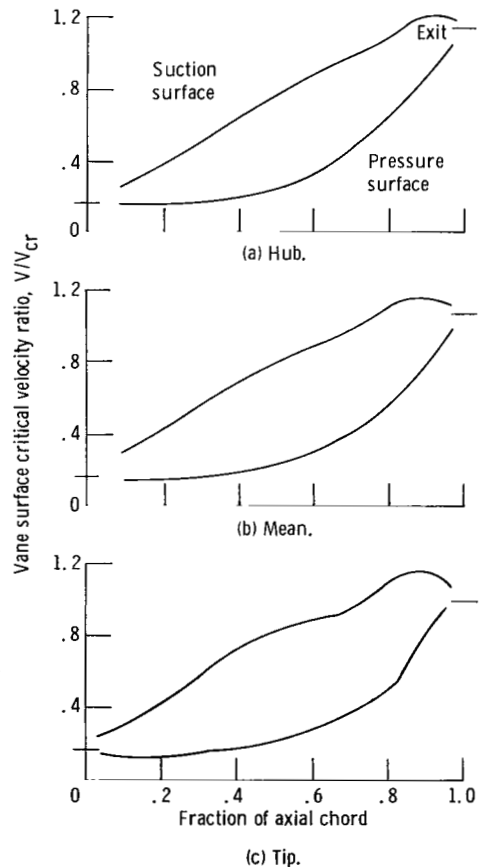


Figure 2. - Design vane surface velocity distribution.

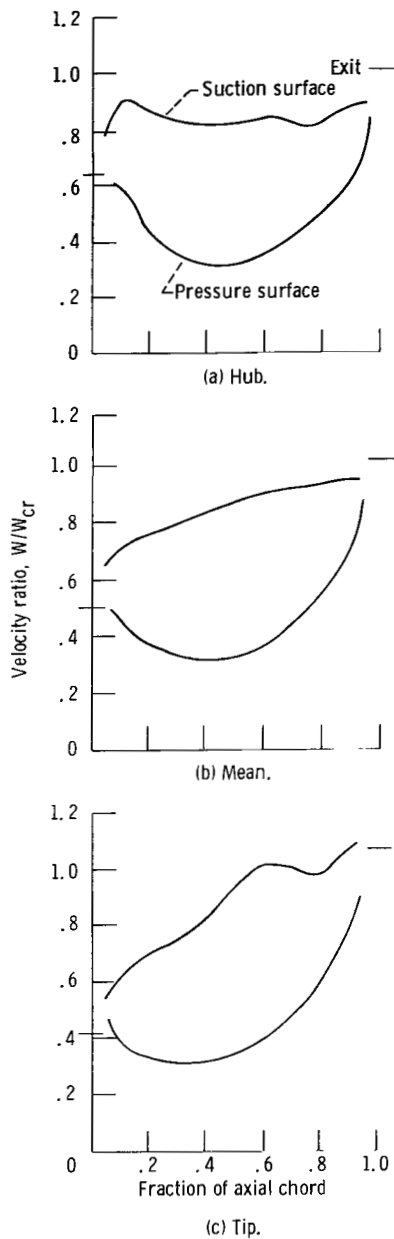


Figure 3. - Design blade surface velocity distributions.

Apparatus

The apparatus consisted of the turbine, as described in the preceding section, a cradled dynamometer, and an inlet and exhaust system with suitable flow control valves. A water-cooled eddy current dynamometer was used to absorb the output power of the turbine, control its speed, and measure

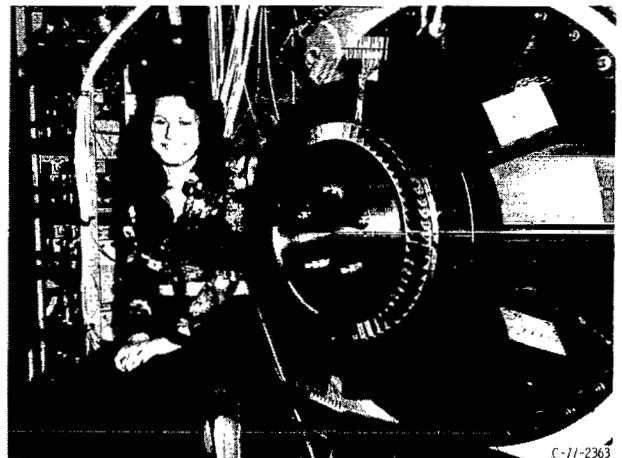


Figure 4. - Stator and rotor installed in test facility.

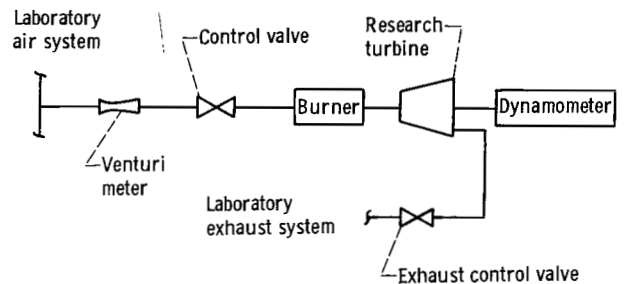


Figure 5. - Basic flow schematic of turbine test facility.

torque output. The dynamometer was supported on hydrostatic bearings to minimize trunnion friction loss. Figure 5 shows the arrangement of the experimental equipment schematically.

The test facility is supplied with dry pressurized air from the laboratory's air system at a pressure of 40 psig and at ambient temperature. The air is ducted through a venturi meter located in a straight section of inlet piping. The inlet pressure is then reduced and controlled by suitable valves in the air lines. The air is then directed to a natural gas vitiated air heater and then through the turbine test section. The turbine exit pressure was set by the use of butterfly control valves in the outlet piping. Figure 6 is a photograph of the test facility.

A schematic cross section of the turbine (fig. 7) also shows the measuring stations where instrumentation is located. The outer casing over the rotor blades incorporated a section of abradable material which was machined to provide a recessed radial clearance of 0.030 cm (0.012 in.).

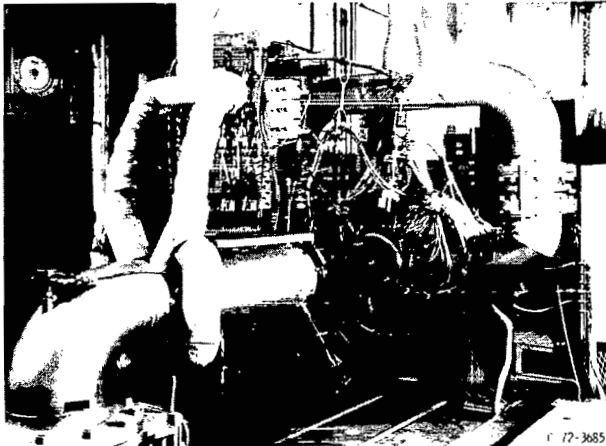
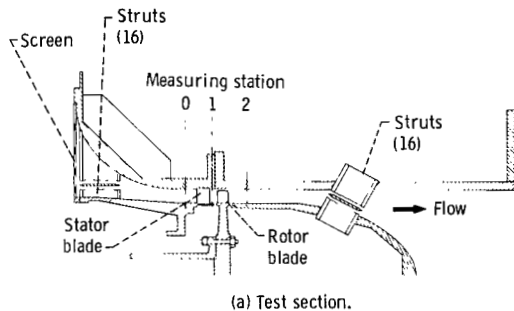
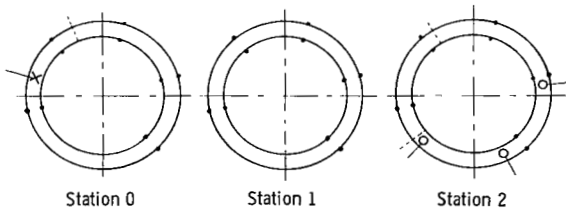


Figure 6. - Turbine test facility.



(a) Test section.

- Wall static-pressure tap
- Thermocouple rake
- Combination angle and total-pressure probe
- × Total-pressure probe



(b) Instrumentation (looking upstream).

Figure 7. - Schematic of turbine test section.

Instrumentation

The type of instrumentation used at each measuring station is shown in figure 7(b). The turbine inlet (station "0") is located 3.78 centimeters (1.49 in.) upstream of the vane leading edge. The instrumentation at the turbine inlet consisted of static

pressure, total pressure and total temperature measuring devices. The inlet temperature was measured with two thermocouple rakes, each containing three thermocouples located at the area center radii of three equal annular areas. Static pressures were obtained from five taps on the inner wall and five taps on the outer wall, as shown in figure 7(b).

Static pressures were measured between the stator and rotor (station "1") by five static taps on both the inner and outer wall, as shown in figure 7(b). In addition to these and not shown on the figure, 17 static taps were equally spaced circumferentially at the tip across two vane exit passages at station "1". These taps were used to measure the static pressure profile downstream of the stator and for comparison with the static pressure predicted analytically.

In addition to the aforementioned stator exit instrumentation, 16 static pressure taps were installed along the hub, mean and tip regions of the stator vane surfaces. The hub and tip taps were 0.152 centimeter (0.060 in.) from the end walls. These static taps were located so as to measure the static pressure distribution along the vane surface from the leading edge to the trailing edge. From these pressures, velocity profiles along the vane surfaces were determined.

At the turbine outlet (station "2") measurements of static pressure, total pressure, total temperature, and outlet flow angles were made. The static pressure was measured with 10 wall taps as described for station "0". The total temperature was measured with two thermocouple rakes, each rake having three thermocouples located at the area center radii of three equal annular areas. The outlet flow angle and total pressure were measured at three circumferential locations as depicted in figure 7(b). Self-aligning probes were used to measure exit total pressures and flow angles.

Data Acquisition

In the primary data acquisition system the pressures were measured by the use of strain gage pressure transducers. The required temperatures were obtained utilizing thermocouples with their output referenced to a suitable fixed precise oven temperature.

The specific work output of the turbine was obtained by measuring speed, torque and mass flow. The speed of the turbine was measured by using an electronic counter in conjunction with a 60-tooth gear mounted on the turbine shaft. A strain gage type load cell was used to measure the torque output of the test turbine. This torque cell was calibrated before and after the test run. Mass flow was

calculated from a universal venturi meter by measuring upstream static pressure and total temperature, and the differential pressure from upstream to the venturi throat.

Each data point consisted of four scans of the data with each scan making up a paragraph. In each scan of data the three exit total pressure probes were located at one of four different radial positions. Each position represented the center of a different equal area segment which when averaged gave an average exit angle for the flow leaving the turbine rotor for use in the equation calculating exit total pressure.

All of the transducer outputs were processed by a microcomputer located in the control room before transmittal to the data collector system located in the laboratory's computer center. These data were then processed based on the prerun torque calibration, and pertinent computed results were sent back to the control room to aid in the judicious selection of test points.

Procedure

Turbine performance was obtained at nominal inlet conditions of pressure and temperature of 24.13 N/cm² (35 psia) and 378 K (680° R), respectively. Data were obtained over a range of inlet- to exit-total pressure ratios from 2.0 to 4.0 and over an equivalent speed range from 60 to 110 percent of design.

The turbine total efficiency was rated on the basis of inlet- to exit-total pressure ratio. Inlet and exit total pressures were calculated from mass flow, static pressure, total temperature, and flow angle by means of the following equation:

$$p' = p \left\{ \frac{1}{2} + \frac{1}{2} \left[1 + \frac{2(\gamma - 1)R}{\gamma g} \left(\frac{w\sqrt{T'}}{pA \cos \alpha} \right)^2 \right]^{1/2} \right\}^{\gamma/(\gamma - 1)}$$

At the inlet, the flow angle was assumed to be axial ($\cos \alpha = 1$). At the exit, the total temperature was computed from measured values of torque, mass flow, and inlet total temperature.

Results and Discussion

The results of this investigation are presented in three parts. The first section covers the turbine performance in terms of mass flow, torque, efficiency and flow angle data together with a performance map. The second section covers measured static pressure distributions along the vane

surface, circumferentially at the vane exit, and across the blade rows. Appropriate comparisons are made to predicted design distributions. Finally, an experimentally determined mean section velocity diagram is presented and compared to the design diagram. All data are shown in terms of "equivalent" air conditions and, for simplicity, the term "equivalent" will be implied and not used in the discussion.

Turbine Performance

Turbine mass flow and torque.—The variation in mass flow with pressure ratio for the speeds tested is shown in figure 8. As noted, the flow choked in the stator at a pressure ratio of about 2.1 with no rotor speed effect. The choking value of 3.856 kilograms per second (8.5 lb/sec) is 4.0 percent higher than the design value of 3.708 kilograms per second (8.175 lb/sec). This difference could be a combination of fabrication tolerances, misalignment of the vanes, or loss assumptions used in the design. It is interesting to note that, at the flat vane exit flow angle involved (73° from axial), this 4 percent excess flow represents a misalignment of the stator vanes of only 0.7°. This underscores the care required in the design and fabrication of high Mach number core turbines with flat vane angles to properly match the turbine to the rest of the engine.

The variation in torque output with pressure ratio for the speeds tested is shown in figure 9. At design speed and pressure ratio, the torque was 348.2 newton-meter (256.8 ft-lb), which is within 2 percent of the limiting loading value of 354.5 newton-meter (261.5 ft-lb).

Overall performance.—The overall turbine performance is shown in figure 10 in terms of specific work output $\Delta h/\theta_{cr}$ as a function of mass flow-speed parameter wNe/δ for lines of constant total pressure ratio and rotor speed. Contours of constant values of total efficiency are also shown.

The turbine efficiency at design speed and pressure ratio (3.44) was 88.6 percent and is indicated by the circle in figure 10. This is 0.6 point lower than the design value of 89.2 percent. This difference could well be within instrument accuracy. Other influencing factors could be the higher than design mass flow with attendant changes in the rotor incidence and reaction, or a greater than design rotor tip clearance. An experimentally determined velocity diagram will be discussed later that shows differences in flow angles and reaction from design values. As mentioned previously, the design clearance was 0.030 centimeter (0.012 in.) and is 0.8 percent of the blade height. Data from references 2 and 8 indicate this difference in efficiency could be accounted for by an

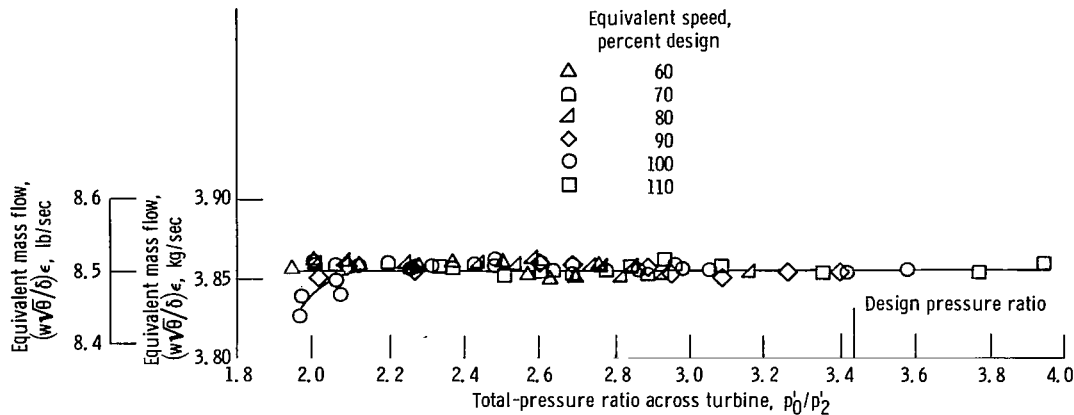


Figure 8. - Variation of equivalent mass flow with total-pressure ratio.

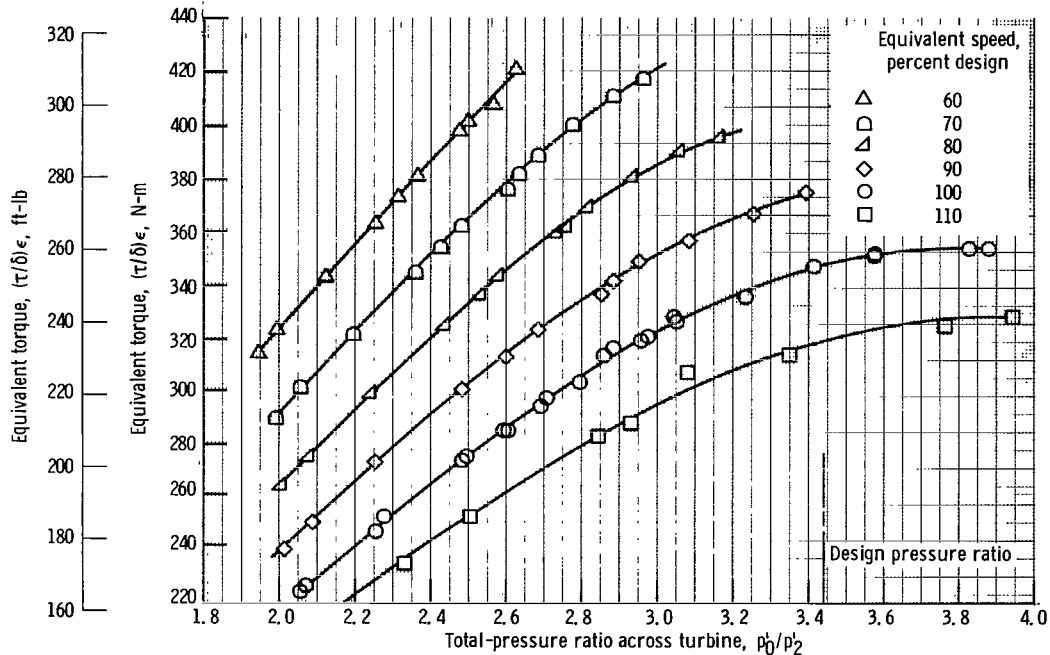


Figure 9. - Variation of equivalent torque with total-pressure ratio.

increase in running clearance of only about 0.013 centimeter (0.005 in.) over the design value. This amounts to a difference in average temperatures of the casing and rotor of less than 20 K (36° R). Unfortunately, running clearances were not measured during the testing procedure. Such measurements should be made to enhance the meaningfulness of aerodynamic test results of core turbines.

Early flow choking and approach to limiting loading at the higher speeds are also noted from figure 10. At intermediate pressure levels, efficiency is seen to be fairly constant for a given speed.

Turbine efficiency.—The variation in efficiency with overall turbine pressure ratio is shown in figure 11 for design speed. The interesting feature of figure 11 is the rapid decrease in efficiency at the higher pressure ratios tested. Efficiency is fairly

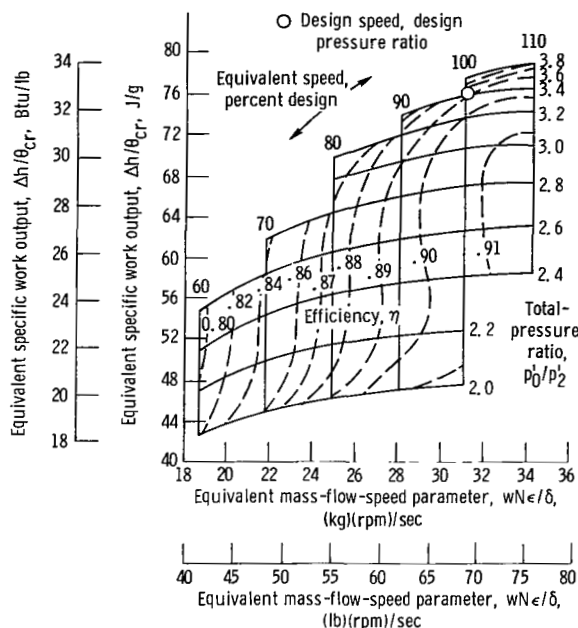


Figure 10. - Performance map.

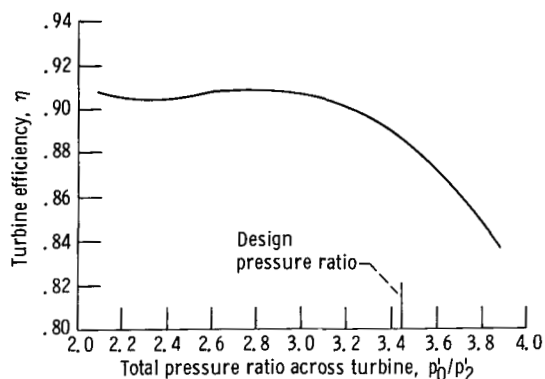


Figure 11. - Variation of efficiency with pressure ratio at design speed.

constant at about 90 to 91 percent for pressure ratios up to about 3.2. It then decreases rapidly to 88 and 84 percent as pressure ratio is increased to 3.5 and 3.85, respectively. This rapid decrease is typical of high Mach number turbines and the reason is attributable to the decreasing payoff in torque output at the higher pressure ratios relative to the increase in ideal work output. This will be amplified later when the variations in static pressure across the blade rows are discussed. As mentioned earlier, turbine efficiency at the design pressure ratio of 3.44 was 88.6 percent.

Exit flow angle.—The variation in turbine exit flow angle as a function of pressure ratio is shown as

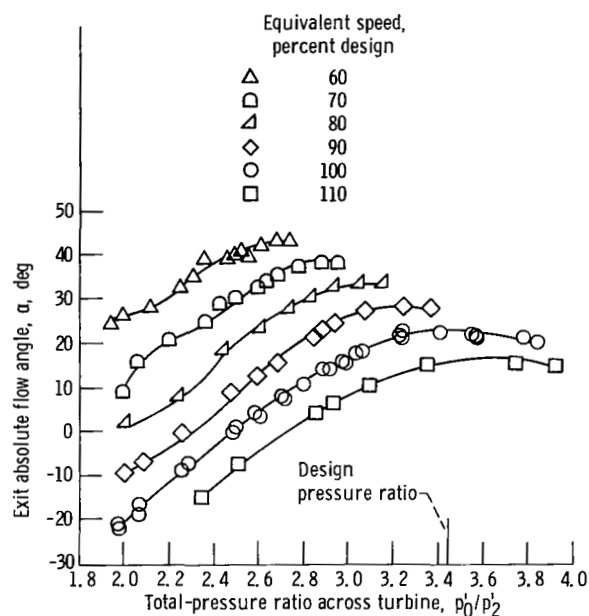


Figure 12. - Variation in turbine exit flow angle with pressure ratio.

figure 12 for the rotor speeds tested. At design speed and work output, the measured average flow angle was 22.6° , which compares favorably to the design average value of 23.7° from the velocity diagrams (fig. 1). This measured value will be used later to construct an experimentally determined velocity diagram.

Static Pressure Distributions

Vane surface velocity distribution.—The experimental velocity distributions were obtained at design speed and pressure ratio from static taps along the vane suction and pressure surfaces at the hub, mean, and tip locations. They are compared to values in figure 13. Good agreement is seen to exist, with experimental velocities slightly lower than design at the hub region, and slightly higher than design at the tip region.

Variation in static pressure across blade rows.—The variations in hub and tip static pressures at the turbine inlet, stator exit, and rotor exit are shown in figure 14 as a function of overall pressure ratio at design speed. The static pressures at the hub and tip of the rotor exit are seen to be nearly equal over the entire range of pressure ratio tested. This is consistent with the small amount of exit swirl shown by the exit flow angle data of figure 12.

The flow conditions at the stator exit were limited by the rotor at overall pressure ratios greater than 3.0. This is evidenced from figure 14 by the constant

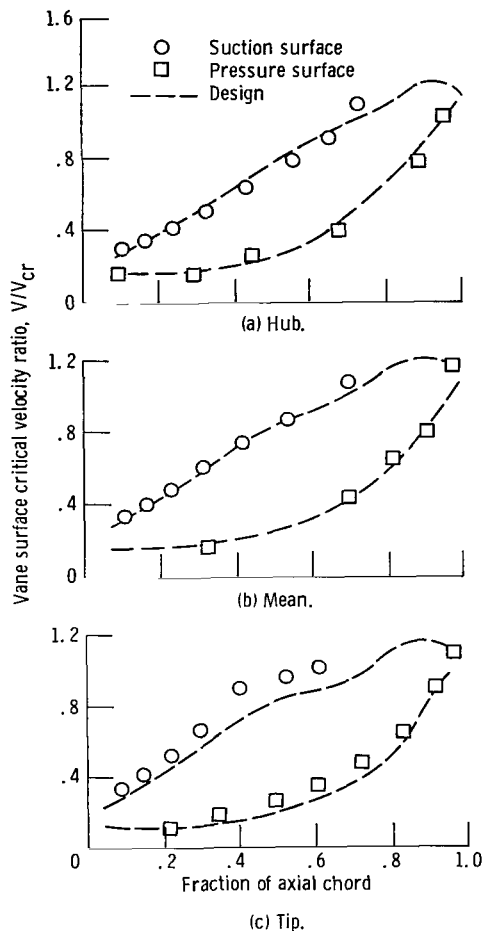


Figure 13. - Comparison of experimentally determined vane surface velocity distributions with design values.

static pressures at the stator exit at both the hub and tip locations. For these conditions, there is no further increase in tangential velocity from the stator exit ($\Delta V_{u,1}$) and increases in actual turbine work output (proportional to ΔV_u) result only from increases in tangential velocity at the rotor exit ($\Delta V_{u,2}$). It is for this reason that turbine efficiency falls off rapidly at high pressure ratios.

In view of the previous discussion, it would be desirable to delay the incipient rapid decrease in efficiency by delaying the point at which no further increase in tangential velocity resulted from the vane. In terms of a design change, this implies a higher Mach number from the vane with less rotor reaction. Although such a design should delay the rapid decrease in efficiency, a new stator-rotor loss analysis would have to be made to predict a net loss or gain at the design point.

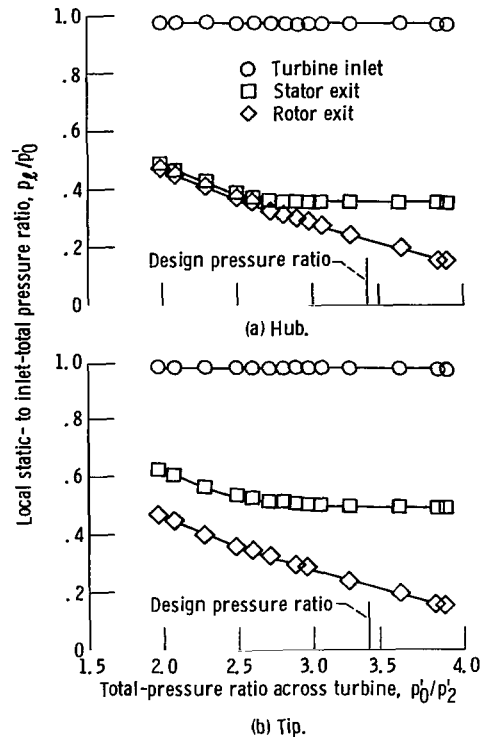


Figure 14. - Variation of static pressure through turbine with pressure ratio at design speed.

Circumferential variation in static pressure at the stator exit.—The variation in tip static pressure at design speed and pressure ratio in a plane 0.63 centimeter (0.25 in.) axially downstream of the vane trailing edge is shown in figure 15. This plane is midway between the vane trailing edges and the blade leading edges. The data behind both passages are superimposed to show repeatability, which is good. Figure 15 indicates a large gradient across the free-stream portion of the passage. This gradient was converted to critical velocity ratio and compared to analytical data obtained from reference 9 and shown in figure 16. There are three analytical planes shown to compare mixing characteristics. One was at the same plane as the static taps, 0.63 centimeter (0.25 in.) downstream of the vanes. The second was considerably downstream, 1.25 centimeter (0.5 in.), and the third was very close to the vane trailing edges, 0.13 centimeter (0.05 in.) downstream. As indicated, very little mixing has occurred in the free-stream region midway between the vanes and blades as compared to theory. This could certainly have an unknown blade incidence loss effect resulting from the unsteady flow conditions entering the rotor. This

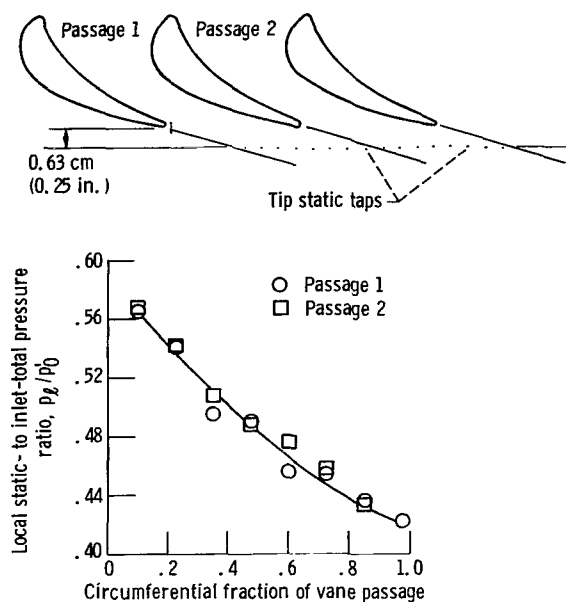


Figure 15. - Circumferential variation in static pressure in a plane 0.63 centimeter (0.25 in.) downstream of vane tip trailing edges at design speed and pressure ratio.

is exemplified by figure 17, which shows the expected change of blade relative inlet flow angle at the tip region for the middle 80 percent of the free-stream passage. The solid curve represents the average design velocity diagram at the tip region. The other two diagrams were obtained from the data from figure 16 and assuming a constant free-stream absolute flow angle α_1 . As indicated in figure 16, a swing in inlet flow angle of over 14° could reasonably be expected to occur every time a blade passes behind a vane passage. The effect of this unsteady flow on blade loss is not known, but it could be significant. It is undoubtedly more influential as vane exit Mach numbers increase with accompanying increases in vane suction surface downstream curvature and relatively thick trailing edges required for cooling.

Experimental Velocity Diagram

A mean radius velocity diagram was calculated using the experimentally obtained values of mass flow, work output, and average outlet flow angle for the condition of design work output at design speed. In this procedure the assumption was made that the work output, mass flow, and flow angle at the mean radius can be taken as the average for the blade row. The rotor outlet velocity was determined from the mass flow, average flow angle, and known total state conditions. The stator outlet velocity was then

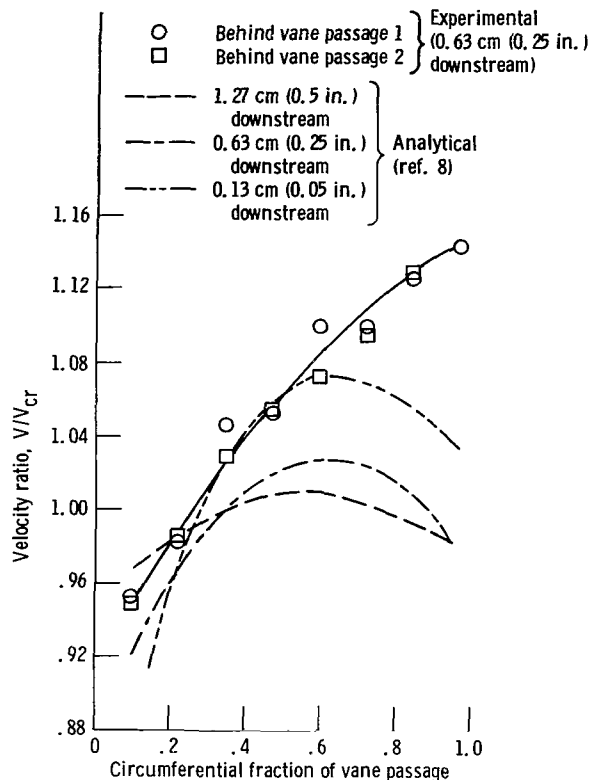


Figure 16. - Comparison of experimentally determined and analytically predicted vane exit critical velocity ratios at the tip region; design speed and pressure ratio.

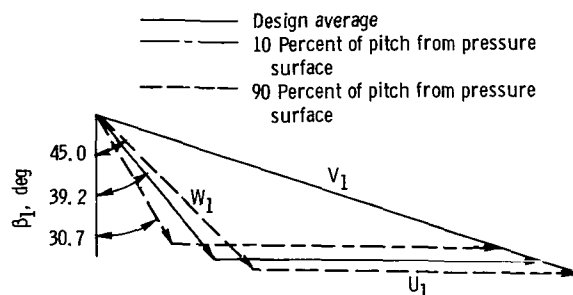
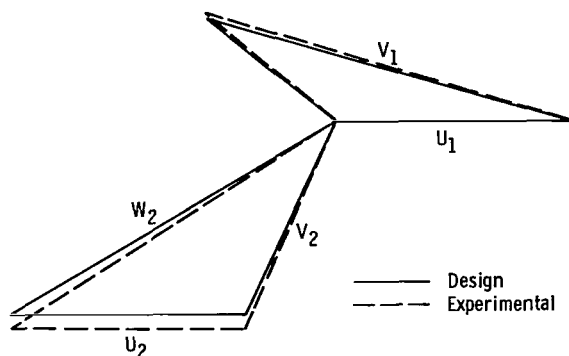


Figure 17. - Circumferential variation in blade tip relative inlet angle in a plane halfway between vane trailing edges and blade leading edges; speed and pressure ratio.

determined from mass flow and known whirl velocity. The resulting diagram is compared with the design velocity diagram in figure 18. As indicated, the angles were slightly opened towards axial due to the 4 percent higher than design mass flow which resulted in a change in blade incidence of about 1.6° . The 0.6 percent deficit in efficiency also resulted in a small increase in rotor reaction of about 1 percent.



	Design value		Experimental value	
	Velocity			
	m/sec	ft/sec	m/sec	ft/sec
$V_{u,1}$	311.2	1020.9	310.1	1017.5
$V_{u,2}$	75.0	246.0	76.0	249.4
$V_{x,1}$	94.8	311.1	99.3	325.8
$V_{x,2}$	166.8	547.3	182.6	599.2
V_1	325.3	1067.3	325.6	1068.3
V_2	182.9	600.0	197.8	649.1
W_1	147.0	482.4	149.1	489.3
W_2	320.6	1051.9	330.0	1082.7
	Angle, deg			
α_1	73.05		72.25	
β_1	49.83		48.26	
α_2	-24.20		-22.60	
β_2	-58.65		-56.40	

Figure 18. - Comparison of design velocity diagram at mean radius with that calculated from experimental results. (All values in table correspond to turbine inlet conditions of U. S. standard sea-level air.)

The small changes in flow angles and reaction from design would not be expected to cause any noticeable difference in turbine losses.

Summary of Results

A solid version of a 50.8-centimeter (20-in.) turbine designed for high temperature core engine applications was tested in cold air. The single-stage turbine was designed for an equivalent specific work output of 76.84 joules per gram (33.01 Btu/lb) at an engine turbine tip speed of 579.1 meters per second (1900 ft/sec). The primary results are summarized as follows:

1. At design speed and pressure ratio, the efficiency was 0.886, which is 0.6 point lower than the design value of 0.892. Contributing causes of this deficit could be an increased blade tip running

clearance over design and a higher than design weight flow. Cold static tip clearance was not measured during test. An increase of only 0.013 centimeter (0.005 in.) would account for the 0.6 point efficiency deficit, and this amounts to a difference in average temperatures of the casing and rotor disk of less than 20 K (36° R). It is highly desirable to measure running clearances during the testing of core turbines to accurately interpret the results.

2. At design speed and pressure ratio, the measured flow was 4.0 percent greater than design. The result was a change in rotor blade incidence of 1.6°, and, together with the 0.6 point deficit in efficiency, resulted in a 1 percent increase in rotor reaction. Because of the flat vane exit flow angle (73° from axial), this 4 percent increase in flow represents a misalignment in vane flow angle of only 0.7°. This underscores the care required in the design and fabrication of high Mach number core turbines with flat vane angles to properly match the turbine to the rest of the engine.

3. Very little mixing occurred in a plane midway between the vanes and blade. This plane was 0.63 centimeter (0.25 in.) axially downstream of the vane trailing edges. Calculations indicate that a rotor blade could experience a pulsating 14° swing in inlet flow angle each time it passed a vane exit. The effect of this unsteady flow on blade incidence loss is unknown, but it could be significant.

4. Design work output and design speed occurred on the rapidly decreasing portion of the efficiency versus pressure ratio curve. A possible design improvement would be to delay the incipient decrease by increasing vane exit Mach number and decreasing blade reaction. A detailed analysis of the new stator-rotor losses would indicate a net loss or gain of such a change.

Lewis Research Center,
National Aeronautics and Space Administration,
Cleveland, Ohio, February 1, 1980,
505-04.

References

1. Szanca, Edward M.; Schum, Harold J.; and Hotz, Glen M.: Research Turbine for High-Temperature Core Engine Application. I—Overall Performance of Solid Scaled Turbine. NASA TN D-7557, 1974.
2. Szanca, Edward M.; Behning, Frank P.; and Schum, Harold J.: Research Turbine for High-Temperature Core Engine Application. II—Effect of Rotor Tip Clearance on Overall Performance. NASA TN D-7639, 1974.
3. McDonel, J.D.; Hsia, E.S.; and Hartsel, J.E.: Core Turbine Aerodynamic Evaluation—Design of Initial Turbine. NASA CR-2512, 1975.

4. Hsia, E.S.; McDonel, J.D.; and Eckert, T.T.: Core Turbine Aerodynamic Evaluation—Design of Second Turbine. NASA CR-2541, 1975.
5. McDonel, J.D.; et al.: Core Turbine Aerodynamic Evaluation—Test Data from Initial Turbine. NASA CR-2596, 1976.
6. Eiswerth, J.E.; et al: Core Turbine Aerodynamic Evaluation: Test Data from Second Cooled Turbine with Combinations of Cooled and Solid Vanes and Blades. NASA CR-2873, 1977.
7. Whitney, Warren J.; Schum, Harold J.; and Behning, Frank P.: Cold-Air Investigation of a 3 1/2 Stage Fan-Drive Turbine with a Stage Loading Factor of 4 Designed for an Integral Lift Engine. II—Performance of 2-, 3-, and 3 1/2-Stage Stage Configurations. NASA TM X-3482, 1977.
8. Haas, Jeffrey E.; and Kofskey, Milton G.: Effect of Rotor Tip Clearance and Configuration on Overall Performance of a 12.77-Centimeter Tip Diameter Axial-Flow Turbine. AVRADCOM TR-78-54, NASA TM-79025, 1978.
9. Katsanis, Theodore: FORTRAN Program for Calculating Transonic Velocities on a Blade-to-Blade Stream Surface of a Turbomachine. NASA TN D-5427, 1969.

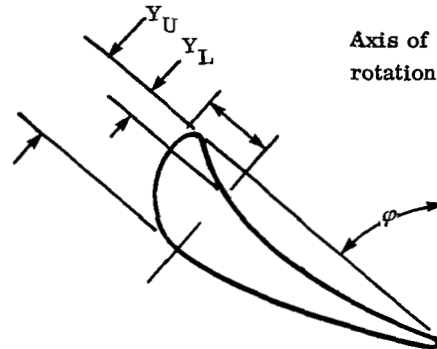
TABLE I. - TURBINE DESIGN OPERATING VALUES

Performance parameter	Hot engine conditions (ASTM-A-1/Air = 0.0435)	Air-equivalent conditions
Inlet total temperature, T_0' , K ($^{\circ}$ R)	2200 (3960)	288.2 (518.7)
Inlet total pressure, p_0' , N/cm ² abs (psia)	386.1 (560)	10.13 (14.7)
Mass flow, w , kg/sec (lbm/sec)	49.41 (108.92)	3.708 (8.175)
Turbine rotative speed, N , rpm	21 772	8081
Specific work output, $\Delta h'$, J/g (Btu/lbm)	557.7 (239.6)	76.84 (33.01)
Blade tip speed, U_t , m/sec (ft/sec)	579.1 (1900)	215 (705.3)
Inlet- to exit-total pressure ratio, p_0'/p_2'	3.00	3.44
Total efficiency, η , percent	0.892	0.892

TABLE II. - TEST TURBINE GEOMETRY

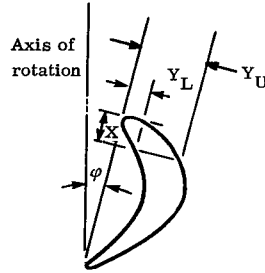
Stator	
Mean diameter, D_{mv} , cm (in.)	46.99 (18.5)
Vane height, b_v , cm (in.)	3.81 (1.5)
Axial chord, c_{xv} , cm (in.)	3.81 (1.5)
Axial solidity, $(c_{xv}/s_v)m$	0.929
Aspect ratio, b_v/c_x	1.000
Number of vanes	36
Leading edge radius, cm (in.)	0.254 (0.100)
Trailing edge radius, cm (in.)	0.0635 (0.025)
Rotor	
Mean diameter, D_{mb} , cm (in.)	46.99 (18.5)
Blade height, b_b , cm (in.)	3.81 (1.5)
Axial chord, c_{xb} , cm (in.)	3.429 (1.35)
Axial solidity, $(c_{xb}/s_b)m$	1.487
Aspect ratio, b_b/c_{xb}	1.111
Number of blades	64
Leading edge radius, cm (in.)	0.1905 (0.075)
Trailing edge radius, cm (in.)	0.0635 (0.025)

TABLE III. - STATOR VANE COORDINATES



All sections					
Orientation angle, $\phi = 48^\circ 38'$					
X		Y_L		Y_U	
cm	in.	cm	in.	cm	in.
0	0	0.254	0.100	0.254	0.100
.127	.05	.033	.013	.925	.364
.254	.10	0	0	1.171	.461
.381	.15	.033	.013	1.336	.526
.508	.20	.127	.050	1.455	.573
.635	.25	.208	.082	1.542	.607
.762	.30	.277	.109	1.608	.633
1.016	.40	.384	.151	1.684	.663
1.270	.50	.462	.182	1.717	.676
1.524	.60	.516	.203	1.717	.676
1.778	.70	.551	.217	1.692	.666
2.032	.80	.574	.226	1.648	.649
2.286	.90	.582	.229	1.593	.627
2.540	1.00	.579	.228	1.527	.601
2.794	1.10	.566	.223	1.321	.572
3.048	1.20	.549	.216	1.369	.539
3.302	1.30	.521	.205	1.278	.503
3.556	1.40	.488	.192	1.181	.465
3.810	1.50	.447	.176	1.080	.425
4.064	1.60	.404	.159	.970	.382
4.318	1.70	.353	.139	.856	.337
4.572	1.80	.300	.118	.737	.290
4.826	1.90	.241	.095	.615	.242
5.080	2.0	.178	.070	.488	.192
5.334	2.1	.114	.045	.358	.141
5.588	2.2	.043	.017	.226	.089
5.715	2.250	.008	.003	.157	.162
5.819	2.291	.064	.025	.064	.025

TABLE IV. - ROTOR BLADE COORDINATES



X		Hub section				Mean section				Tip section			
Orientation angle, φ													
9° 46'						14° 15'				18° 44'			
		Y _L		Y _U		Y _L		Y _U		Y _L		Y _U	
cm	in.	cm	in.	cm	in.	cm	in.	cm	in.	cm	in.	cm	in.
0	0	0.1981	0.078	0.1981	0.078	0.1880	0.074	0.1880	0.074	0.1854	0.073	0.1854	0.073
.0254	.01	.0864	.034	.3658	.144	.0838	.033	.3505	.138	.0762	.030	.3327	.131
.0508	.02	.0483	.019	.4775	.188	.0483	.019	.4470	.176	.0432	.017	.4140	.163
.0762	.03	.0254	.010	.5690	.224	.0254	.010	.5283	.208	.0229	.009	.4851	.191
.1016	.04	.0127	.005	.6426	.253	.0127	.005	.5944	.234	.0102	.004	.5512	.217
.127	.05	.0051	.002	.7087	.279	.0051	.002	.6528	.257	.0025	.001	.6096	.240
.1905	.075	.0025	.001	.8306	.327	.0051	.002	.7849	.309	.0051	.002	.7391	.291
.254	.100	.0279	.011	.9271	.365	.0305	.012	.8865	.349	.0279	.011	.8407	.331
.3175	.125	.0787	.031	1.0185	.401	.0762	.030	.9779	.385	.0737	.029	.9347	.368
.381	.150	.1499	.059	1.0973	.432	.1397	.055	1.0541	.415	.1321	.052	1.0160	.400
.508	.200	.2946	.116	1.2268	.483	.2718	.107	1.1938	.470	.2489	.098	1.1557	.455
.635	.250	.4191	.165	1.3335	.525	.4623	.152	1.3005	.512	.3505	.138	1.2675	.499
.762	.300	.5258	.207	1.4199	.559	.4826	.190	1.3868	.546	.4394	.173	1.3589	.535
.889	.350	.6147	.242	1.4884	.586	.5613	.221	1.4580	.574	.5131	.202	1.4300	.563
1.016	.400	.6858	.270	1.5418	.607	.6274	.247	1.5138	.596	.5740	.226	1.4834	.584
1.143	.450	.7442	.293	1.5799	.622	.6833	.269	1.5519	.611	.6299	.248	1.5240	.600
1.270	.500	.7874	.310	1.6027	.631	.7239	.285	1.5748	.620	.6655	.262	1.5494	.610
1.397	.550	.8204	.323	1.6104	.634	.7518	.296	1.5824	.623	.6909	.272	1.5621	.615
1.524	.600	.8357	.329	1.6053	.632	.7696	.303	1.5773	.621	.7087	.279	1.5570	.613
1.651	.650	.8407	.331	1.5824	.623	.7798	.307	1.5621	.615	.7188	.283	1.5418	.607
1.778	.700	.8357	.329	1.5469	.609	.7772	.306	1.5291	.602	.7188	.283	1.5164	.597
1.905	.750	.8230	.324	1.4986	.590	.7671	.302	1.4859	.585	.7137	.281	1.4757	.581
2.032	.800	.7976	.314	1.4376	.566	.7442	.293	1.4326	.564	.6960	.274	1.4224	.560
2.159	.850	.7620	.300	1.3589	.535	.7163	.282	1.3665	.538	.6731	.265	1.3589	.535
2.286	.900	.7188	.283	1.2725	.501	.6782	.267	1.2903	.508	.6426	.253	1.2878	.507
2.413	.950	.6655	.262	1.1786	.464	.6350	.250	1.2040	.474	.6071	.239	1.2065	.475
2.540	1.000	.6045	.238	1.0795	.425	.5817	.229	1.1074	.436	.5588	.220	1.1176	.440
2.667	1.050	.5359	.211	.9754	.384	.5237	.206	1.0033	.395	.5105	.201	1.0185	.401
2.794	1.100	.4597	.181	.8636	.340	.9804	.180	.8890	.350	.4572	.180	.9169	.361
2.921	1.150	.3785	.149	.7442	.293	.3861	.152	.7947	.305	.3962	.156	.8052	.317
3.048	1.200	.2896	.114	.6147	.242	.3073	.121	.6502	.256	.3277	.129	.6934	.273
3.175	1.250	.1930	.076	.4801	.180	.2235	.088	.5207	.205	.2591	.102	.5766	.227
3.302	1.300	.0914	.036	.3327	.131	.1321	.052	.3861	.152	.1829	.072	.4496	.177
3.429	1.350	0	.000	.1753	.069	.0330	.013	.2438	.096	.0991	.039	.3200	.126
3.500	1.378	.0635	.025	.0635	.025	-----	-----	-----	-----	-----	-----	-----	-----
3.556	1.400	-----	-----	-----	-----	.0457	.018	.0838	.033	.0051	.002	.1854	.073
3.561	1.402	-----	-----	-----	-----	.0635	.025	.0535	.025	-----	-----	-----	-----
3.647	1.436	-----	-----	-----	-----	-----	-----	-----	-----	.0635	.025	.0635	.025

1. Report No. NASA TP-1680		2. Government Accession No.		3. Recipient's Catalog No.	
4. Title and Subtitle DESIGN AND COLD-AIR TEST OF SINGLE-STAGE UNCOOLED CORE TURBINE WITH HIGH WORK OUTPUT				5. Report Date June 1980	
				6. Performing Organization Code	
7. Author(s) Thomas P. Moffitt, Edward M. Szanca, Warren J. Whitney, and Frank P. Behning				8. Performing Organization Report No. E-316	
				10. Work Unit No. 505-04	
9. Performing Organization Name and Address National Aeronautics and Space Administration Lewis Research Center Cleveland, Ohio 44135				11. Contract or Grant No.	
				13. Type of Report and Period Covered Technical Paper	
12. Sponsoring Agency Name and Address National Aeronautics and Space Administration Washington, D.C. 20546				14. Sponsoring Agency Code	
15. Supplementary Notes					
16. Abstract A solid version of a 50.8-cm (20-in.) single-stage core turbine designed for high temperature was tested in cold air over a range of speed and pressure ratio. Design equivalent specific work was 76.84 J/g (33.01 Btu/lb) at an engine turbine tip speed of 579.1 m/sec (1900 ft/sec). At design speed and pressure ratio, the total efficiency of the turbine was 88.6 percent, which is 0.6 point lower than the design value of 89.2 percent. The corresponding mass flow was 4.0 percent greater than design.					
17. Key Words (Suggested by Author(s)) Turbine aerodynamic High specific work			18. Distribution Statement Unclassified - unlimited STAR Category 07		
19. Security Classif. (of this report) Unclassified		20. Security Classif. (of this page) Unclassified		21. No. of Pages 17	
				22. Price* A02	

National Aeronautics and
Space Administration

SPECIAL FOURTH CLASS MAIL
BOOK

Postage and Fees Paid
National Aeronautics and
Space Administration
NASA-451



Washington, D.C.
20546

Official Business
Penalty for Private Use, \$300

6 1 1U,A, 061380 S00903DS
DEPT OF THE AIR FORCE
AF WEAPONS LABORATORY
ATTN: TECHNICAL LIBRARY (SUL)
KIRTLAND AFB NM 87117

NASA

POSTMASTER: If Undeliverable (Section 158
Postal Manual) Do Not Return
